

Modifications of Surfactant Distributions and Surface Morphologies in Latex Films Due to Moisture Exposure

Guizhen H. Xu,[†] Jinping Dong,[‡] Steven J. Severtson,^{*,†} Carl J. Houtman,[§] and Larry E. Gwin^{||}

Department of Bioproducts and Biosystems Engineering, University of Minnesota, 2004 Folwell Avenue, St. Paul, Minnesota 55108, Characterization Facility, University of Minnesota, 12 Shepherd Laboratories, 100 Union Street S.E., Minneapolis, Minnesota 55455, USDA, Forest Products Laboratory, One Gifford Pinchot Drive, Madison, Wisconsin 53726, and Franklin International, 2020 Bruck Street, Columbus, Ohio 43207

Received: March 25, 2009; Revised Manuscript Received: June 6, 2009

Migration of surfactants in water-based, pressure-sensitive adhesive (PSA) films exposed to static and cyclic relative humidity conditions was investigated using confocal Raman microscopy (CRM) and atomic force microscopy (AFM). Studied PSA films contain monomers *n*-butyl acrylate, vinyl acetate, and methacrylic acid and an equal mass mixture of anionic and nonionic nonylphenol ethoxylate emulsifiers. A leveling of surfactant concentration distributions is observed via CRM after films stored at 50% relative humidity (RH) are exposed to a 100% RH for an extended time period, while relatively small increases in surface enrichment occur when films are stored at 0% RH. Use of CRM for binary mixtures containing anionic or nonionic surfactant and latex that has undergone dialysis to remove nonpolymeric components indicates that surfactant–polymer compatibility governs to a great extent surface enrichment, but not changes observed with humidity variations. AFM images show that upon drying latex coatings, surfactant and other additives collect in large aggregation regions, which protrude from film surfaces. These structures are absent at high humidity, which appears to result from lateral spreading across the polymer surface. When humidity is reduced, aggregation regions reform but appear to be smaller and more evenly dispersed, and by cycling humidity between 0 and 100% RH, interfacial enrichment can be seen to diminish. Presented results provide greater insights into the distribution behavior of surfactants in latex films and potential mechanisms for observed issues arising for these systems.

Introduction

Surfactants are introduced to water-borne pressure-sensitive adhesive latexes during emulsion polymerization to control both particle size and stability of formed dispersions. However, inclusion of surfactants, which are generally low molecular weight compounds (<1000 g/mol), can have adverse effects on water resistance and performance properties of adhesives.^{1–6} These are caused by the fact that surfactant often concentrates in aggregates at film surfaces during water evaporation and formation.^{7–11} Surfactant exudation upon latex film formation has been reported to occur toward film–air and/or film–substrate interfaces to produce a distribution of local surfactant concentrations.^{12–17} It is also possible that surfactant species can migrate beyond adhesive surfaces to contaminate an adjacent ply in an adhesive laminant, for example, facstock in label constructions. Although it is now well accepted that surfactants can concentrate at adhesive surfaces during coating processes, the mechanism involved is not well understood, and thus neither is the subsequent movement and eventual fate of these species in adhesive films.

It has been reported that the main factors influencing migration of surfactants to interfaces during film formation include chemical composition and structural characteristics of

both surfactants and adhesive polymers and temperature.^{18,19} During coating processes, water is drawn to the surface and evaporates, carrying with it and concentrating solutes. Thus, it is likely that the tendency of surfactant species to collect at film surfaces is governed to a large extent by their partitioning between aqueous (continuous) and polymer phases. This behavior that is indicated by measures of surfactant hydrophobicity, such as critical micelle concentration, hydrophilic–lipophilic balance, octanol–water distribution coefficient, and pK_a values for acidic functional groups.^{19–21} In a previous publication, the authors demonstrated the significantly greater tendency of the anionic form of a nonylphenol ethoxylate surfactant to concentrate at the surface of an acrylic water-based PSA versus that of its nonionic form. The difference was attributed to the greater hydrophilicity of the anionic species due to its ionized acid functional group(s). The importance of temperature in this process has been discussed by several authors. For example, Aramendia et al. reported an unexpectedly large amount of conventional surfactant was exuded to film surfaces when annealed at a temperature above the glass transition temperature of the polymer, as compared to reactive surfactants (surfmers).²² Scalarone et al. reported similar results demonstrating that aging at temperatures much higher than the polymer glass transition temperature promoted diffusion of surfactants to film surfaces.²³

Here, results from an examination of the role of humidity on surfactant migration are discussed. Surfactant distributions in PSA films will likely govern to a great extent their interactions with moisture, thus characterizing this relationship is important to understanding how environmental conditions used for storage impact performance of pressure-sensitive (PS) products. As part

* Corresponding author. Phone: (612) 625-5265. Fax: (612) 625-6286. E-mail: sever018@umn.edu.

[†] Department of Bioproducts and Biosystems Engineering, University of Minnesota.

[‡] Characterization Facility, University of Minnesota.

[§] Forest Products Laboratory.

^{||} Franklin International.

of this study, films were cast and aged under various environmental conditions, and movements of the surfactant species were monitored via atomic force microscopy (AFM) and confocal Raman microscopy (CRM). The combination of these techniques for this purpose was introduced in a recent article.¹⁹ Past characterization of this mechanism relied almost exclusively on attenuated total reflectance-Fourier-transform infrared or ATR-FTIR spectroscopy.^{12,14–18,20,24–28} While this is effective at identifying the presence of the surfactant at the interface, it does not provide information on the overall distribution. Confocal Raman microscopy (CRM) measures the Raman spectra for a small volume of film without any modification of samples by combining a high resolution confocal microscope with a sensitive Raman spectroscopy system, providing a powerful method for the depth profiling of thin films, coatings, membranes, and composites.^{19,29,30} Application of CRM, especially near interfaces, and fitting of data with an exponential decay model provide for quantitative analysis of surfactant distributions at both film–air and film–substrate interfaces. Introduction of AFM phase images further elucidates the redistribution mechanism by providing an image of how surfactants interact with moisture and the impact this has on film surface morphology.

Experimental Section

Materials. A water-based PSA based on commercial formulations was synthesized at Franklin International (Columbus, OH) from the monomers *n*-butyl acrylate, vinyl acetate, and methacrylic acid and a combination of an anionic surfactant, disodium ethoxylated nonylphenol half ester of sulfosuccinic acid (50 mass %), and a nonionic surfactant, nonylphenoxy poly(ethyleneoxy) ethanol (50 mass %). The solids content of produced latex was 60–63 mass % with a mean particle size of 690 nm diameter obtained via dynamic light scattering technique. The total surfactant content in films assuming complete retention is approximately 0.025 mmol/g (1.8 mass %), and the glass transition temperature determined via dynamic mechanical analysis is $-34\text{ }^{\circ}\text{C}$. Adhesive films of 1 mil (25.4 μm) thicknesses were generated by coating latex onto a 60 lb (60 lbs of mass per 3000 ft^2 or 97.7 g/m^2) silicone-coated release linear using a wire wound rod and drying it in an $82\text{ }^{\circ}\text{C}$ oven for 10 min. These so-called “draw-down” films were covered with an 80 lb (130 g/m^2) silicone-coated release linear for migration experiments. PSA draw-down films were kept at 50% RH and $22\text{ }^{\circ}\text{C}$ for several months on wire shelving prior to being cut into 1 in. strips and introduced into environmental jars containing desiccant (0% relative humidity or RH) and water (100% RH) for long-term (60 days) storage and humidity cycling tests. Spin-coated films were cast by spin coating PSA latex on 15 mm AFM specimen disks under ambient conditions. These films had a thickness of approximately 10 μm and were used for AFM imaging in an environmental chamber.

Confocal Raman Microscopy. An alpha 300R confocal Raman microscope equipped with a UHTS200 spectrometer and a DV401 CCD detector from WITec (Ulm, Germany) was employed to collect single Raman spectra from PSA films. A Nikon 100 \times oil immersion objective was used for all measurements. An Ar-ion laser with the wavelength of 514.5 nm and maximum power of 50 mW was used for excitation. Lateral resolution of the confocal Raman microscope according to the theory of light diffraction is about 250 nm, and vertical resolution is about 500 nm. Because the sampling volume may be smaller than the average particle size of the latex spheres, measurements were conducted at several random locations on the film to minimize the variation. Raman spectra of film

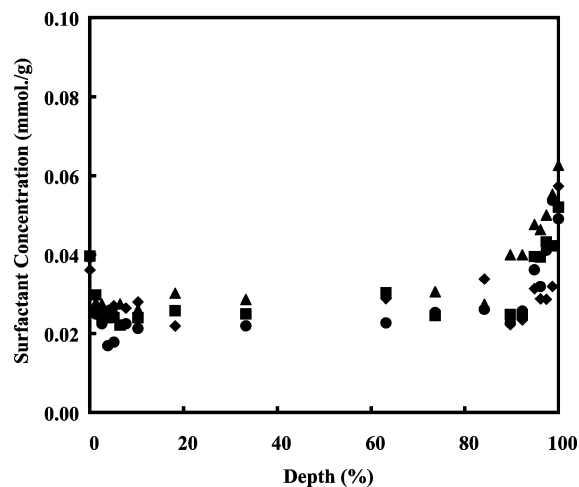


Figure 1. Surfactant distribution profiles of original PSA film, which was stored at $22\text{ }^{\circ}\text{C}$ and 50% RH. 0% corresponds to the film–air interface and 100% to the film–substrate interface. Four depth profiles are shown as indicated by the different markers.

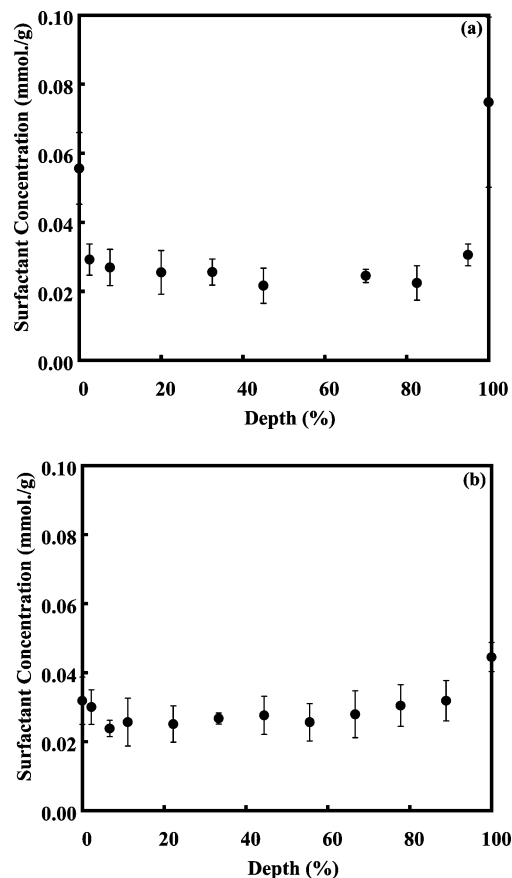


Figure 2. Surfactant distribution profiles of PSA film after being aged for 2 months at $22\text{ }^{\circ}\text{C}$ and (a) 0% RH and (b) 100% RH. (Again, 0% corresponds to the film–air interface and 100% to the film–substrate interface.)

samples were recorded with the integration time of 240 s and laser power of 30 mW. Peaks at 1612 and 1735 cm^{-1} are assigned to an aromatic C–C, on-ring stretch mode for the surfactant, and carbonyl stretch mode of the polymer, respectively.¹⁹ Calibration was carried out with standards produced from the adhesive polymer and pure surfactant. Polymer was isolated through dialysis of the latex and dissolution in tetrahydrofuran (THF).

TABLE 1: Parameters from Fit with Exponential Decay Model for Surfactant Distributions of Model PSA Films at 22 °C and Relative Humidity of 0 and 100%

| interface | parameters | 50% RH ^a | 0% RH | 100% RH |
|----------------|---------------------------------|---------------------|--------|---------|
| film–air | C_0 (mmol/g) | 0.0248 | 0.0257 | 0.0242 |
| | A (mmol/g) | 0.0151 | 0.0284 | 0.0081 |
| | α (μm^{-1}) | 2.87 | 1.89 | 0.56 |
| film–substrate | C_0 (mmol/g) | 0.0257 | 0.0240 | 0.0262 |
| | A (mmol/g) | 0.0308 | 0.0495 | 0.0180 |
| | α (μm^{-1}) | 0.528 | 0.99 | 0.19 |

^a Original sample stored at 50% RH.**TABLE 2: Enrichment Factors for PSA Films**

| interface | 50% RH | 0% RH | 100% RH |
|----------------|--------|-------|---------|
| film–air | 0.609 | 1.10 | 0.335 |
| film–substrate | 1.198 | 2.06 | 0.68 |

Atomic Force Microscopy (AFM). Atomic force microscopy (AFM) was used to examine the variation of surface morphologies of PSA films with relative humidity. Using a Molecular Imaging PicoPlus PicoSPM 3000 (now Agilent Technology, Santa Clara, CA, model 5500) system, AFM imaging was performed in an environmental chamber with controlled temperature and relative humidity (RH). Intermittent contact or tapping mode AFM was utilized. The principles and detailed information concerning this application of AFM are provided elsewhere.¹⁹ For the AFM phase images presented here, the cantilever was operated in the repulsive regime with free oscillation amplitude of 300 nm and $A/A_0 \approx 0.9$ –0.95, in which the viscous or more energy dissipative material produces a dark contrast on the phase image, while stiff or less energy dissipative materials provide bright contrast. Integrated silicon cantilevers with tip radii of curvature 5–10 nm were employed in AFM imaging. The spring constant of the cantilever was manufacturer-specified in the range of 30–60 N/m, and the measured resonant frequency was within 10% of 300 kHz. AFM imaging of the spin-coat PSA films was conducted at ambient temperature (22–24 °C) but at various relative humidity levels from 3% RH to 90% RH. To guarantee that an AFM image is representative, the measurements were conducted at least two times, imaging different regions of the same film sample.

Results and Discussion

Surfactant Migration under Constant Humidity Conditions. Figure 1 shows surfactant concentration distributions or depth profiles for the original PSA films, which had been stored at 50% RH and 22 °C after drying. Analysis using CRM was carried out on four randomly selected coatings. The samples all have thicknesses of about 1 mil (24.5 μm) and show similar surfactant concentration profiles, in which surfactant enrichments at the film–substrate interface are higher than those at the film–air interface, and bulk phase concentrations of the surfactant blend are close to the added concentration of 0.025 mmol/g. (Draw-down PSA films were analyzed from the film–air interface with 0% corresponding to the film–air

interface and 100% to the film–substrate interface.) In Figure 2, plots of averaged depth profile data are shown for film samples stored for 60 days and at 22 °C at 0% RH (Figure 2a) and 100% RH (Figure 2b). Each point is an average calculated for five or more measurements. It can be seen that the depth profile for the sample stored under dry conditions appears to show a slightly greater enrichment at the interfaces, especially at the film–substrate interface. In contrast, samples stored at 100% RH show a more even distribution of surfactant. It was noted that the thicknesses of PSA films after being aged at 100% RH for 2 months were found to be approximately 30% greater than those of films aged at 0% RH for the same period.

More direct Raman analyses of interfaces were carried out on the adhesive films. These involved multiple measurements within about the first 5 μm of film surfaces where differences in surfactant concentrations are observed. It was shown previously that these surface distribution curves are well fit by the exponential decay model,¹⁹ that is,

$$C(z) = C_0 + A \exp(-\alpha z) \quad (1)$$

where $C(z)$ is surfactant concentration at a depth z from the interface, C_0 is the bulk phase surfactant concentration, and A and α are fitting constants indicating the maximum enrichment of surfactant and rate of decay, respectively. The fitting parameters are listed in Table 1 along with those for the samples aged at 0 and 100% RH for 60 days. (For all PSA films, r^2 values for the model fits were >0.92 .) For the purpose of monitoring the impact of humidity on surfactant distributions, eq 1 is modified to the form

$$C(z)/C_0 = 1 + \kappa \exp(-\alpha z) \quad (2)$$

where κ is equal to A/C_0 and defined as the enrichment factor. This dimensionless parameter indicates the increased surface concentration of a surfactant relative to the bulk. Enrichment factors for the original samples and those aged for 2 months are listed in Table 2. It can be seen that, in general, storage at 100% RH significantly decreases the enrichment factor at both interfaces, while storage at 0% RH increases it. This would indicate that the presence of moisture or the direction the moisture flows determines whether the surfactant enrichment is enhanced or diminished. It also appears that there is a greater change in the enrichment factor at the film–substrate interface than that at the film–air interface. It is possible that this difference may result from the design of the storage laminate. As discussed above, PSA films are produced by coating the latex onto a 60 lb release liner (defined as the substrate), drying the coating in an oven to form the adhesive film, and then covering it with an 80 lb liner. The 60 and 80 lb liners have measured water vapor transmission rates of 710 g/m^2 day versus 488 g/m^2 , respectively. Thus, we would expect a greater movement of moisture through the film–substrate interface.

Surfactant Migration with Humidity Cycling. From the results presented above, it appears that surfactant enrichment

TABLE 3: Enrichment Factors for PSA Films Aged at 22 °C Under Various Humidity Conditions

| interface | two cycles, conditioned at 0% RH for 1 day | conditioned at 0% RH for 5 days | dissolved in THF, conditioned for 1 day | |
|----------------|--|---------------------------------|---|---------|
| | | | 0% RH | 100% RH |
| film–air | 0.494 | 0.626 | 0.575 | 0.564 |
| film–substrate | 0.663 | 1.955 | 0.602 | 0.546 |

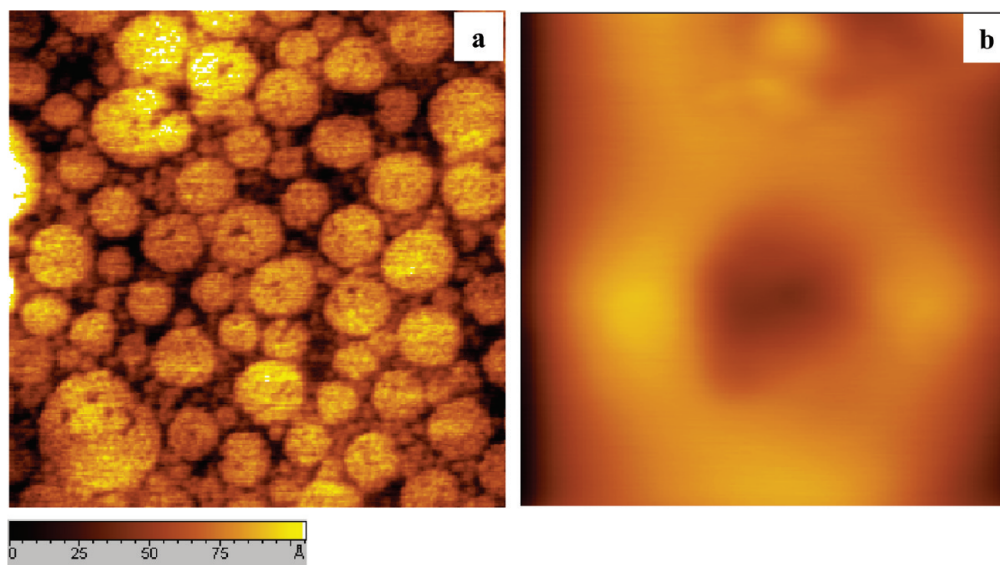


Figure 3. AFM height images of the surface of (a) PSA film showing its residual latex structure and (b) film produced by first dissolving dried latex components in THF (scanning size $5\ \mu\text{m} \times 5\ \mu\text{m}$).

at interfaces is dependent on moisture. What is not clear from the static humidity tests is the mechanism involved. In this section, results for the movement of surfactants in PSA films exposed to humidity cycling are reviewed. Each 48 h cycle involves aging of a PSA film at $22\ ^\circ\text{C}$ in 0% RH for 24 h and then at $22\ ^\circ\text{C}$ and 100% RH for an additional 24 h. The purpose of this study is to help determine if surfactants simply migrate with the moisture flux or if there are changes in the form of surfactant aggregation regions, latex film, or some combination that is being observed.

Table 3 lists enrichment factors from surfactant distributions for both adhesive interfaces exposed to two full humidity cycles and then dried. The table also shows κ values for interfaces of films stored solely at 0% RH and $22\ ^\circ\text{C}$ over the same time period. There are increases in the surface enrichment for films stored under static conditions for 5 days at 0% RH, but they are smaller than those found for films stored under the same conditions for 60 days. In contrast, samples exposed to humidity cycling demonstrate a reduction in the enrichment factor at both interfaces. Another interesting phenomenon associated with this study is the reduction in variation of concentration measurements. For example, standard deviations associated with the first cycles were about 1.0%; by the end of the second cycle, they were 0.30%.

It appears that humidity cycles produce a more even distribution of surfactant species, as well as changes in the structure of PSA films. It was previously reported that surfactant aggregation regions tend to locate in interstitial regions at PSA film surfaces.¹⁹ To gauge the impact of residual latex structure on surfactant distribution, a film was cast in which the structure was eliminated. This was accomplished by dissolving the PSA in tetrahydrofuran (THF) and coating the solution on a 60 lb release liner, which was then dried and covered with an 80 lb liner. Figure 3 shows AFM height images for the top surfaces of PSA and solvent cast films. It is clear that the latex structure, which is retained at the interface in PSA films (Figure 3a), is absent at the surface of solvent cast film (Figure 3b). Surfactant enrichment values from fits of CRM data with eq 2 after solvent cast films were aged in 0% RH and 100% RH and $22\ ^\circ\text{C}$ for 1 day are also listed in Table 3. It can be seen that surfactant enrichment at interfaces of solvent cast films is lower than what would be expected for latex aged under the same conditions.

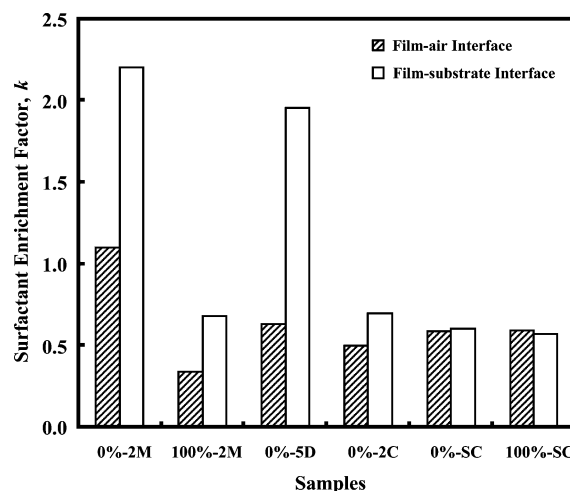


Figure 4. Enrichment factors at both interfaces for PSA films aged at $22\ ^\circ\text{C}$ under various humidity conditions, including 0% and 100% RH for 60 days (0%-2M and 100%-2M, respectively), 0% RH for 5 days (0%-5D), 2 humidity cycles and 0% RH for 1 day prior to testing (0%-2C), and solvent cast films stored at 0% and 100% RH for 1 day (0%-SC and 100%-SC, respectively).

Surfactant enrichments at both interfaces of aged samples are summarized in Figure 4. There clearly exists a move toward a more even distribution of surfactant.

Figure 5 shows AFM height and phase images of film–air interfaces from a PSA film obtained in a humidity chamber at ambient temperatures. The film is exposed to a cycle that begins with equilibration at 25% RH (Figure 5a). The RH is then raised to 90% for equilibration (1 h) (Figure 5b) and then reduced back to 25% RH (Figure 5c). For PSA at low RH, the bright regions around the latex particles are thought to be regions of surfactant and other species such as inorganic salts. The brightness of these regions relative to the dark background, which is composed of latex polymer, indicates a more elastic substance. These aggregates are spread over the entire film but reside primarily in the interstitial regions between latex particles. Average roughness, R_a , obtained from the AFM topographs (shown in Figure 5, middle) is 58 nm, and this appears to be due to the aggregated materials. (Cross-sectional analyses along the white lines are shown below the height images.) Raising

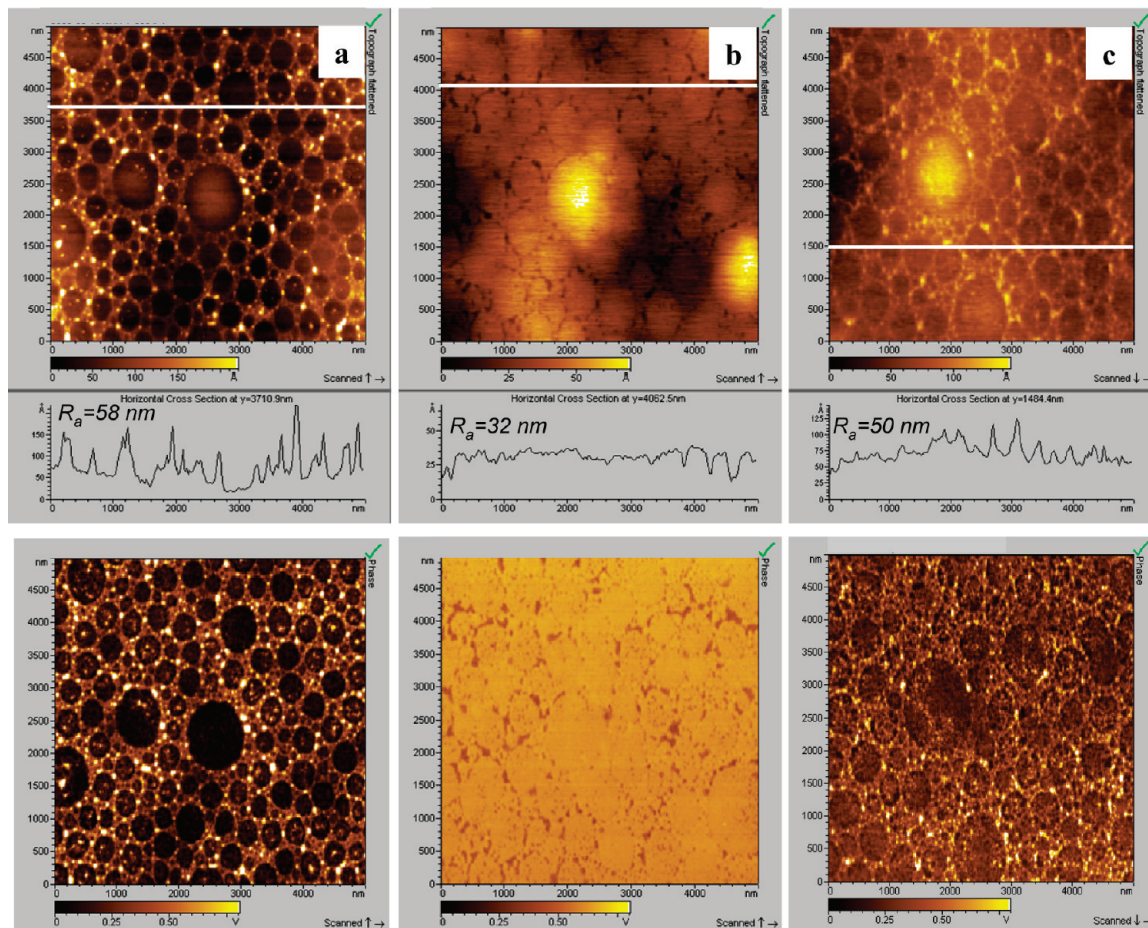


Figure 5. AFM images of PSA film surface obtained at (a) 22 °C and 25% RH, (b) 22 °C and 90% RH, and (c) dried from 90% RH to 25% RH at 22 °C (upper, height images; bottom, phase images).

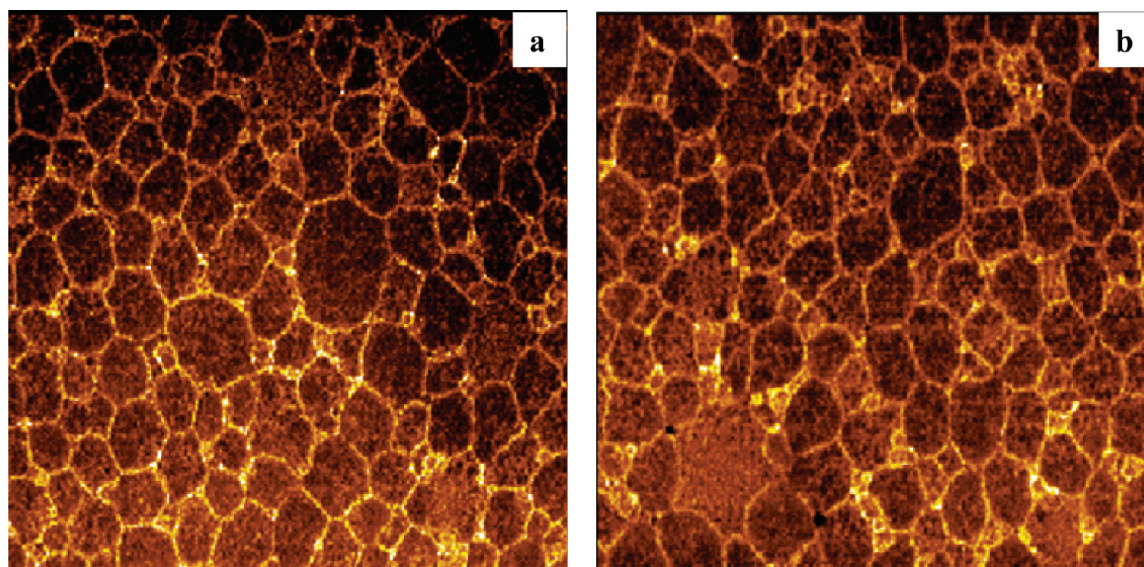


Figure 6. AFM phase images acquired for the latex film subsequent to rinsing with ethanol (~ 3 mL) at 22 °C and (a) 3% RH and (b) 90% RH (scanning size: $5 \mu\text{m} \times 5 \mu\text{m}$).

the relative humidity to 90% RH appears to show the dispersion of the aggregation regions over the entire film. This is consistent with the lower measured R_a , which is 32 nm, nearly one-half its original value. The phase contrast image for the film after the humidity chamber was brought back to 25% RH over a short time frame is shown in Figure 5c. Once again, a distribution of bright specks has developed, but they now appear to be more

evenly distributed and R_a increases to 50 nm, slightly lower than the initial value. More telling are the phase images of the solvent-rinsed PSA film obtained at RH levels of 3% and 90%, respectively (as shown in Figure 6). It can be seen that for the rinsed PSA film—air interface, the phase contrasts did not change with the variation of moisture, and the roughness is low, $R_a = 34$ nm.

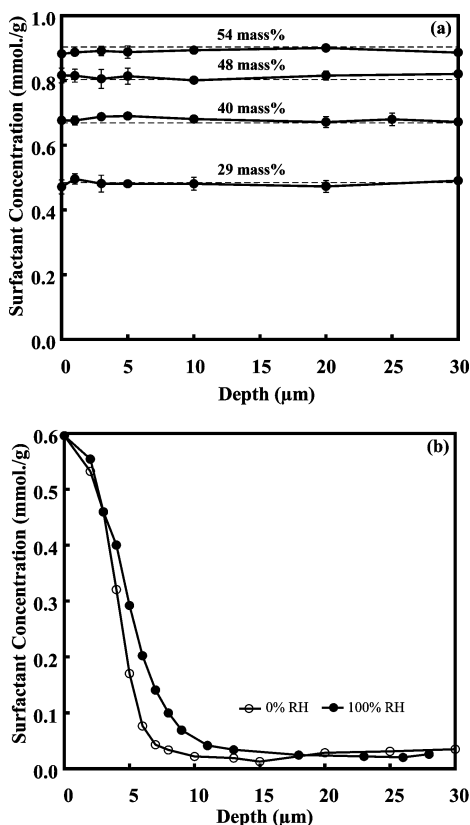


Figure 7. Distribution of (a) nonionic surfactant and (b) anionic surfactant with polymer phase isolated from the latex using dialysis.

Surfactant and Polymer Phase Intermixing. From the results above, it appears that exposure of the PSA films to high humidity results in the lateral migration of surfactant from aggregates formed during the coating and drying process. This is evident from the AFM images, and it also appears to influence the CRM data. The apparent reduction in the enrichment factor at high humidity could indicate that vertical migration of surfactant is occurring. To test for this possibility, experiments were carried out in which pure surfactant was placed on the surface of PSA films and films were aged under extreme humidity conditions. For these experiments, dialysis was carried out on the commercial PSA to remove most of the existing surfactant in the formulation. The latexes were then used to cast films to which anionic and nonionic surfactant were added, and samples were stored in 0% and 100% RH containers at 22 °C for 1 day.

Figure 7a shows the concentration profiles of the nonionic surfactant in adhesive films aged at both 0 and 100% RH. No difference was observed between samples aged at the different humidities, so values were averaged. Surfactant was added at levels up to 54 mass % in the latex following dialysis. The dotted line indicates the concentrations of surfactant added. It can be seen that the amount added becomes evenly distributed throughout the film, even at these high concentrations. Thus, it appears to be highly compatible with the latex polymer, and this compatibility is not affected by different humidity levels. Although readdition of surfactant subsequent to dialysis could conceivably produce differences in contact between surfactants and latex particles, these differences would be expected to lessen the degree of interactions and are a stricter test for compatibility. This result indicates that changes in the surfactant distributions are due primarily to the behavior of the anionic species.

Attempts to generate a curve similar to Figure 7a by adding anionic surfactant to dialyzed PSA latex produced significant

variations in surfactant concentrations throughout the film and increasing interfacial enrichment with greater surfactant addition. This led to an alternative approach in which dried anionic surfactant was applied to the film–air interface of films cast from the dialyzed sample. Figure 7b shows a plot of surfactant concentration versus film depth for the anionic surfactant, which was dried and placed on PSAs and stored at both 0 and 100% RH for 24 h. The interface between the nearly pure surfactant layer and film can be clearly identified for 0% RH but is more diffuse under the high humidity conditions. It is evident that the anionic surfactant is much less compatible and also appears to be unaffected by changes in humidity. For both humidity levels, curves plateau near concentrations added during synthesis, approximately 0.01 mmol/g. From this, it might be concluded that enrichment is governed to a large extent by surfactant–polymer compatibility. However, given the complexity of these systems, further study is necessary. With regard to the vertical movement of the surfactant, the diffuse interface is consistent with the greater mobility of the surfactant. In other words, it is possible that the surfactant's migration under high humidity conditions may include its movement to occupy surface area throughout the interfacial region, as well as penetrating several micrometers into the film.

Summary and Conclusions

Measurements using CRM indicate significant enrichments of nonylphenol ethoxylate, anionic surfactant at interfaces of water-based acrylic PSAs when stored at 0% RH for an extended time period, and a more even distribution when stored at 100% RH. However, concentration measurements recorded for confocal planes at the surface of films are highly variable for samples stored under the low humidity conditions. Cycling the films between 0% RH (24 h) and 100% RH (24 h) produced a more even distribution of surfactant at interfaces and a substantially reduced variability in measurements. Similar results were also obtained when films were dissolved in THF and cast. AFM topographs show that surfactant aggregates protrude from the surface of films cast from latex emulsions, which is primarily responsible for the measured surface roughness. With exposure to high humidity, aggregates are no longer distinguishable, and the phase contrast of the film surface is reversed. Also, surface roughness is diminished to levels measured when the surfactant is removed. Upon returning to low humidity conditions, aggregates are again apparent, but as a greater number of smaller domains, which are more evenly distributed. It is speculated that the enhanced mobility of the surfactant at high humidity and formation of smaller, more evenly distributed aggregates are responsible for the observed reduction in the enrichment factor at 100% RH and subsequent to humidity cycling, respectively. Although film compatibility is a factor determining interfacial enrichment, it does not appear affected by changes in humidity. Future work will examine structure in which surfactant materials are held in the latex polymer as well as the spreading behavior observed on polymer surfaces for high humidity, which is of practical interest as a potential mode of transfer between films and adjacent phases and materials such as facestocks used in label constructions.

Acknowledgment. This research was financially supported in part by a grant from the U.S. Postal Service, Stamp Acquisition and Distribution, and the U.S. Department of Energy Project Number DE-FC36-04GO14309.

References and Notes

- (1) Staicu, T.; Micutz, M.; Leca, M. *Prog. Org. Coat.* **2005**, *53*, 56–62.

- (2) Charmeau, J. Y.; Berthet, R.; Gringreau, C.; Holl, Y.; Kientz, E. *J. Adhes.* **1997**, *17*, 169–176.
- (3) Tobing, S. D.; Klein, A. *J. Appl. Polym. Sci.* **2001**, *79*, 2230–2244.
- (4) Mulvihill, J.; Toussaint, A.; Wilde, M. D. *Prog. Org. Coat.* **1997**, *30*, 127–139.
- (5) Donkus, L. J. *Adhes. Age* **1997**, *32*, 35–37.
- (6) Yang, Y.; Li, H.; Wang, F. *J. Adhes. Sci. Technol.* **2003**, *17*, 1741–1750.
- (7) Wheeler, O. L.; Jaffe, H. L.; Wellman, N. *Off. Dig.* **1954**, *26*, 1239–1241.
- (8) Keddie, J. L. *Mater. Sci. Eng.* **1997**, *3*, 101–170.
- (9) Morizur, J. F.; Irvine, D. J.; Rawlins, J. J.; Mathias, L. J. *Macromolecules* **2007**, *40*, 8938–8946.
- (10) Amalvy, J. I.; Unzue, M. J.; Schoonbrood, H. A. S.; Asua, J. M. *J. Polym. Sci., Part A: Polym. Chem.* **2002**, *40*, 2994–3000.
- (11) Aramendia, E.; Barandiaran, M. J.; Grade, J.; Blease, T.; Asua, J. M. *Langmuir* **2005**, *21*, 1428–1435.
- (12) Zhao, C. L.; Holl, Y.; Pith, T.; Lambla, M. *Colloid Polym. Sci.* **1987**, *265*, 823–829.
- (13) Evanson, K. W.; Urban, M. W. *J. Appl. Polym. Sci.* **1991**, *42*, 2287–2296.
- (14) Evanson, K. W.; Thorstenson, T. A.; Urban, M. W. *J. Appl. Polym. Sci.* **1991**, *42*, 2297–2307.
- (15) Amalvy, J. I.; Soria, D. B. *Prog. Org. Coat.* **1996**, *28*, 279–283.
- (16) Juhue, D.; Wang, Y.; Lang, J.; Leung, O.-M.; Goh, M. C.; Winnik, M. A. *Polym. Mater. Sci.* **1995**, *73*, 86–87.
- (17) Guigner, D.; Fischer, C.; Holl, Y. *Langmuir* **2001**, *17*, 6419–6425.
- (18) Holl, Y. *Macromol. Symp.* **2000**, *151*, 473–478.
- (19) Xu, G. H.; Dong, J.; Severtson, S. J.; Houtman, C. J.; Gwin, L. E. *J. Phys. Chem. B* **2008**, *112*, 11907–11914.
- (20) Kientz, E.; Dobler, F.; Holl, Y. *Polym. Int.* **1994**, *34*, 125–134.
- (21) Lam, S.; Hellgren, A. C.; Sjoberg, M.; Holmberg, K.; Schoonbrood, H. A. S.; Unzue, M. J.; Asua, J. M.; Tauer, K.; Sherrington, D. C.; Montoya Goni, A. *J. Appl. Polym. Sci.* **1997**, *66*, 187–198.
- (22) Aramendia, E.; Mallegol, J.; Jeynes, C.; Barandiaran, M. J.; Keddie, J. L.; Asua, J. M. *Langmuir* **2003**, *19*, 3212–3221.
- (23) Scalarone, D.; Lazzari, M.; Castelvetro, V.; Chiantore, O. *Chem. Mater.* **2007**, *19*, 6107–6113.
- (24) Miller, C. M.; Barnes, H. W. *Proc. Adhes. Soc. Annu. Meeting* **2001**, *24*, 153.
- (25) Kientz, E.; Holl, Y. *Colloids Surf., A* **1993**, *78*, 255–270.
- (26) Belaroui, F.; Hirn, M. P.; Grohens, Y.; Marie, P.; Holl, Y. *J. Colloid Interface Sci.* **2003**, *261*, 336–348.
- (27) Urban, M. W. *Prog. Org. Coat.* **1997**, *32*, 215–229.
- (28) Tebelius, L. K.; Urban, M. W. *J. Appl. Polym. Sci.* **1995**, *56*, 387–395.
- (29) Belaroui, F.; Grohens, Y.; Boyer, H.; Holl, Y. *Polymer* **2000**, *41*, 7641–7645.
- (30) Schmidt, U.; Hild, S.; Ibach, W.; Hollricher, O. *Macromol. Symp.* **2005**, *230*, 133–143.

JP902716B